

Supporting Information

Efficient narrowband yellow organic light-emitting diodes based on iridium(III) complexes with rigid indolo[3,2,1-*jk*]carbazole unit

Qi-Ming Liu¹, Xiao-Jia Liu, Xiao-Sheng Zhong¹, Zhong-Zhong Huo¹, Zhen Shen,¹ and You-Xuan Zheng^{1,2*}

¹State Key Laboratory of Coordination Chemistry, Jiangsu Key Laboratory of Advanced Organic Materials, School of Chemistry and Chemical Engineering, Nanjing University, Nanjing 210023, P. R. China. E-mail: yxzheng@nju.edu.cn

² MaAnShan High-Tech Research Institute of Nanjing University, MaAnShan, 238200, P. R. China.

S1. General measurement

NMR measurements were conducted on a Bruker AM 400 spectrometer. High resolution electrospray mass spectra (HRMS) were measured on G6500 from Agilent for complexes. Ultraviolet-visible absorption and photoluminescence spectra were measured on a UV-3100 spectrophotometer and a Hitachi F-4600 photoluminescence spectrophotometer, respectively. Cyclic voltammetry measurements were conducted on a MPI-A multifunctional electrochemical system (Xi'an Remex Analytical Instrument Ltd. Co., China) at room temperature, with glassy carbon electrode as the working electrode, polished platinum wire electrode as the counter electrode and Ag-AgNO₃ (0.1 M) in CH₃CN as the reference electrode, *tetra-n*-butylammonium perchlorate (0.1 M) as the supporting electrolyte, ferrocene as the standard substance, the scan rate was 0.1 V/s. The photoluminescence quantum yields (PLQYs) were measured with Edinburgh FLS920 fluorescence spectrometer equipped vis an integrating sphere and the decay lifetimes (τ) of the compounds were measured with HORIBA FL-3 fluorescence spectrometer. Thermogravimetric analysis (TGA) was performed on a Pyris 1 DSC under nitrogen atmosphere at a heating rate of 10 °C min⁻¹. The single crystal of complex was carried out on a Bruker SMART CCD diffractometer using monochromated Mo Ka radiation ($\lambda = 0.71073 \text{ \AA}$) at room temperature. Cell parameters were retrieved using SMART software and refined using SAINT on all observed reflections.

S2. OLEDs fabrication and measurement

All OLEDs were fabricated on the pre-patterned ITO-coated glass substrate with a sheet resistance of 15 Ω sq⁻¹. The deposition rate for organic compounds is 1-2 Å s⁻¹. The phosphor and the host (mCBP) were co-evaporated to form emitting layer from two separate sources. The cathode consisting of LiF/Al was deposited by evaporation of LiF with a deposition rate of 0.1 Å s⁻¹ and then by evaporation of Al metal with a rate of 3 Å s⁻¹.

The characteristic curves of the devices were measured with a computer controlled KEITHLEY 2400 source meter with a calibrated silicon diode in air without device encapsulation. Based on the uncorrected PL and EL spectra, CIE coordinates were calculated using a test program of the Spectra scan PR650 spectrophotometer. The EQE of EL devices were calculated based on the photon energy measured by the photodiode.

S3. NMR and HRMS spectra

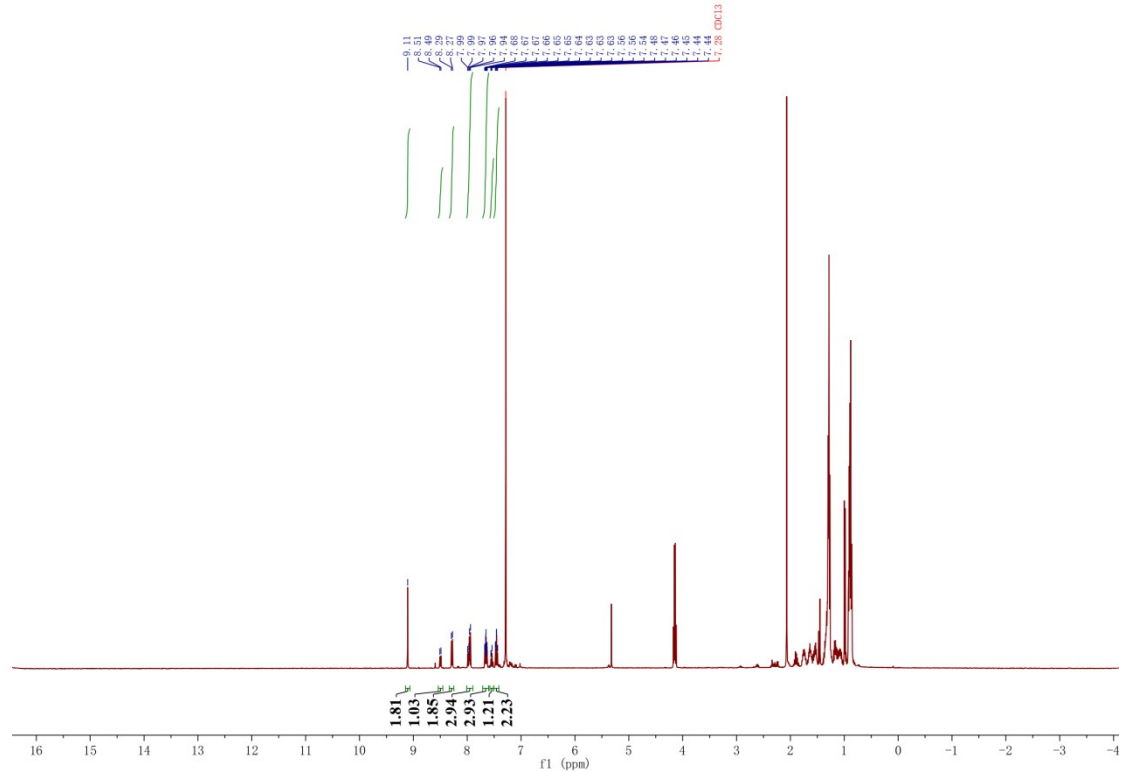


Fig. S1 ^1H NMR spectrum of PhthzICz in CDCl_3 .

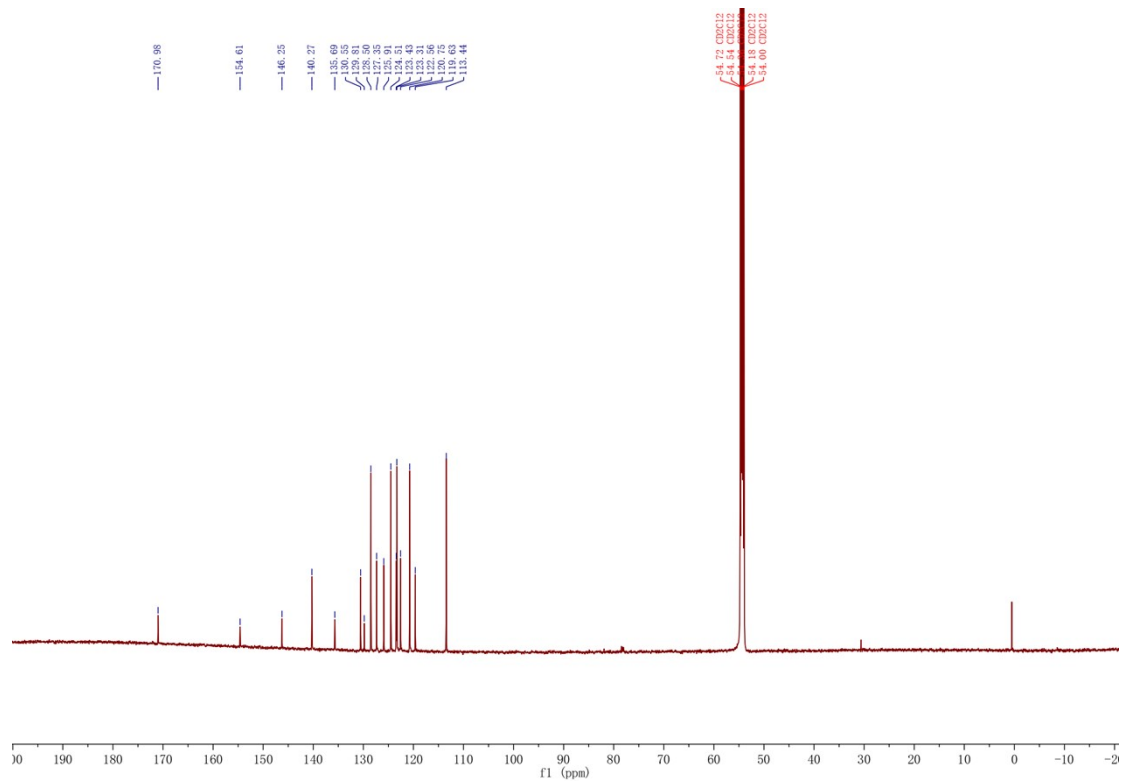


Fig. S2 ^{13}C NMR spectrum of PhthzICz in CDCl_3 .

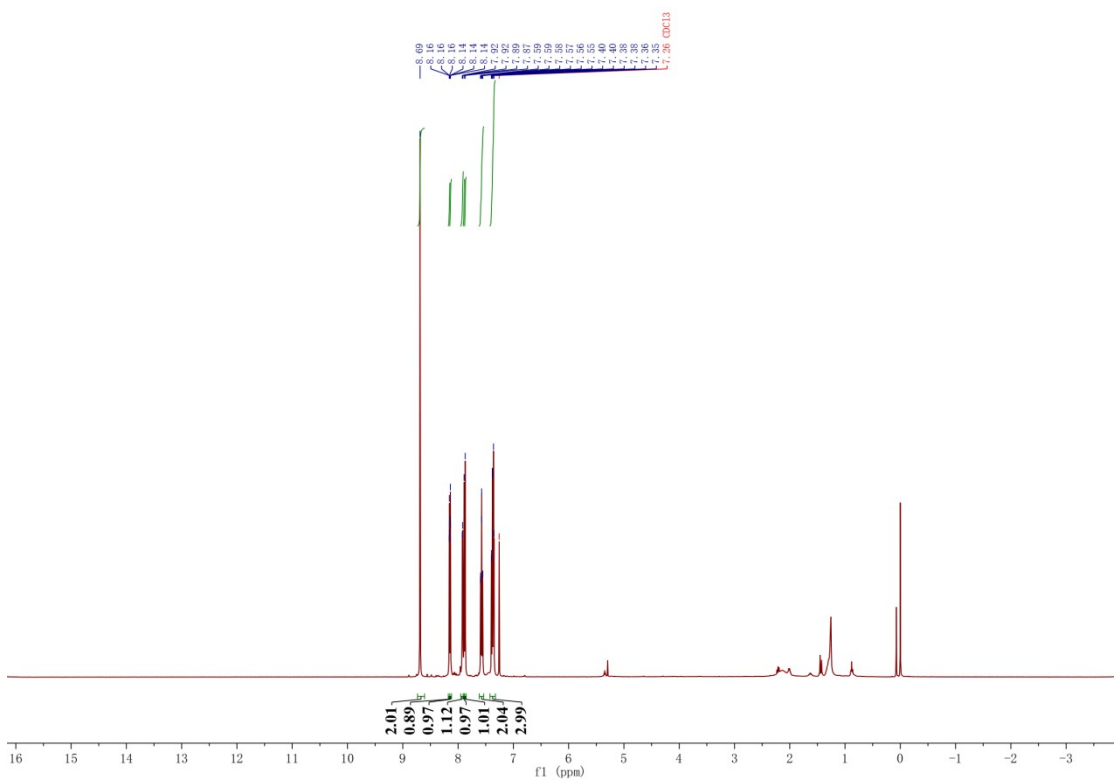


Fig. S3 ^1H NMR spectrum of thzICz in CDCl_3 .

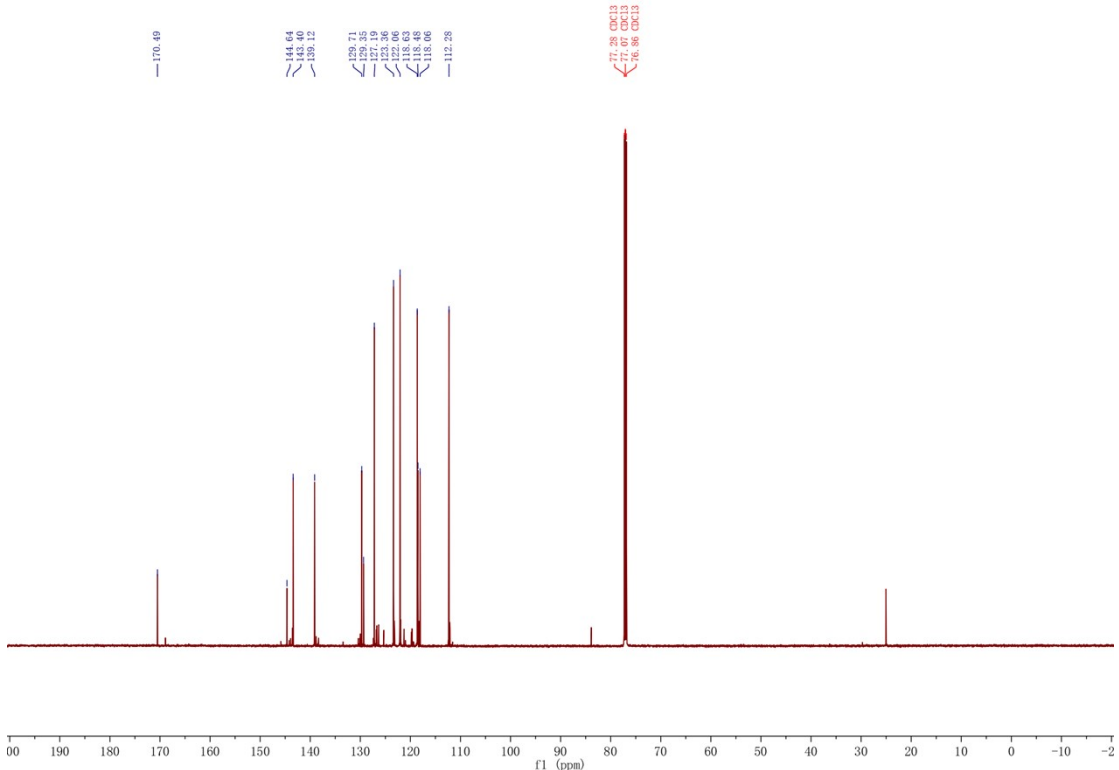


Fig. S4 ^{13}C NMR spectrum of thzICz in CDCl_3 .

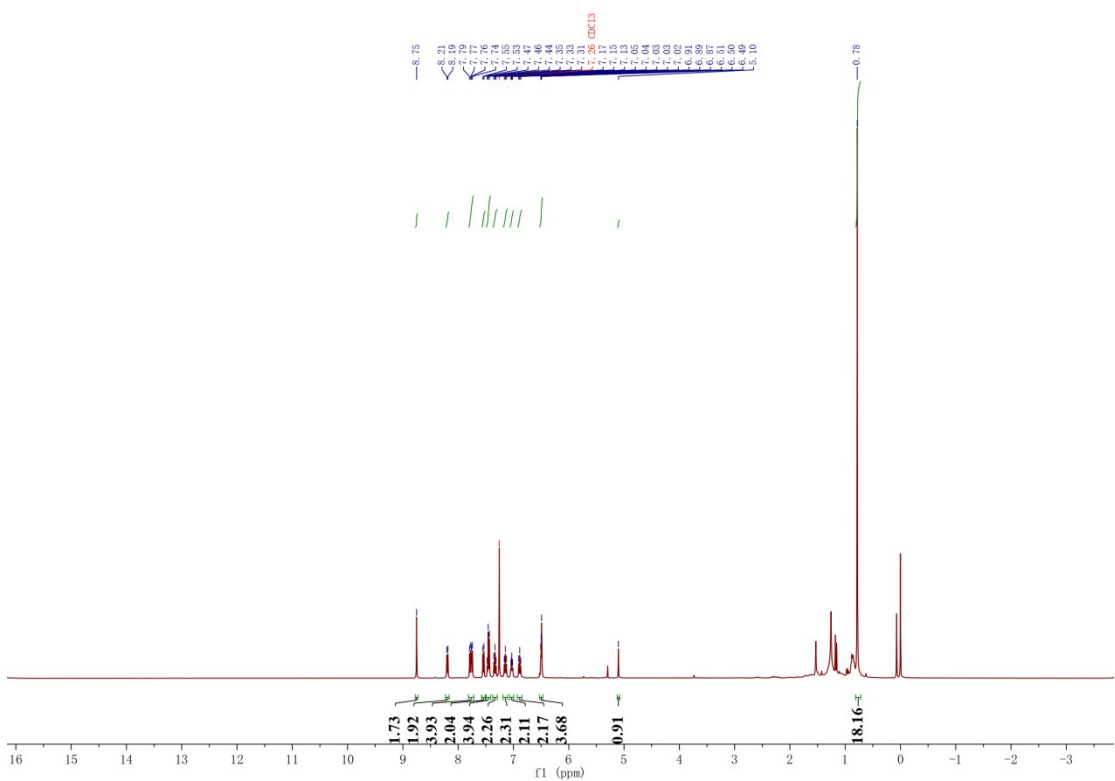


Fig. S5 ^1H NMR spectrum of $(\text{PhthzICz})_2\text{Ir}(\text{tmd})$ in CDCl_3 .

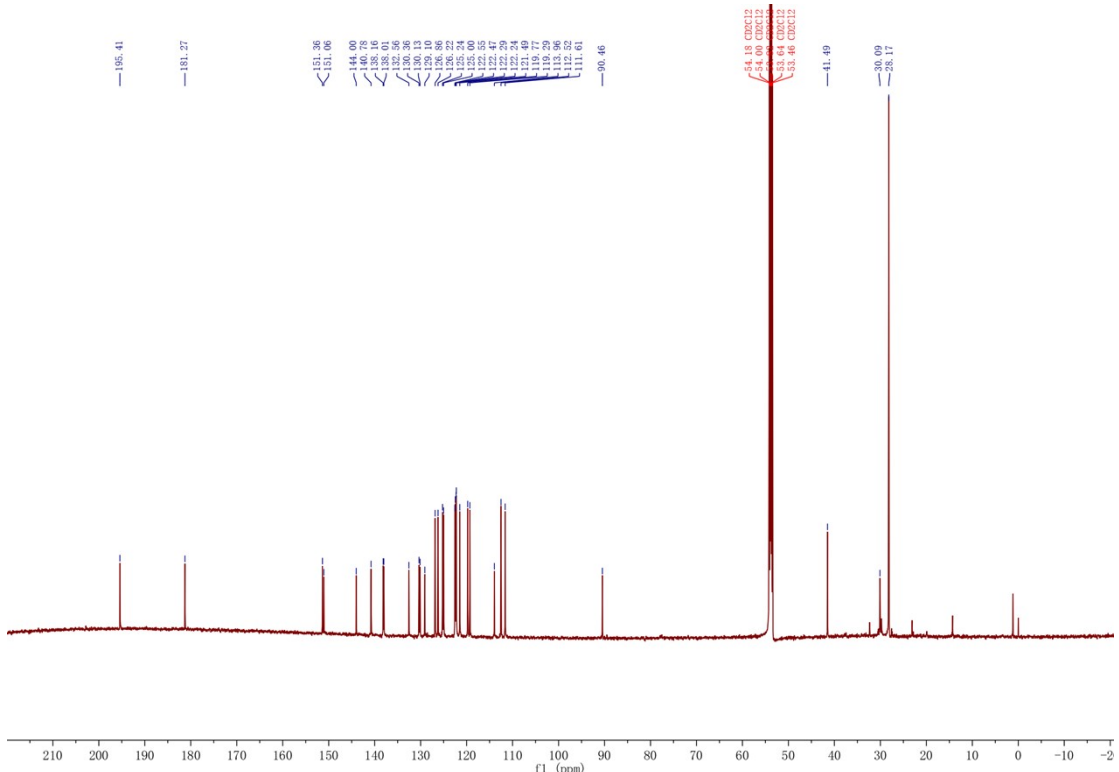


Fig. S6 ^{13}C NMR spectrum of $(\text{PhthzICz})_2\text{Ir}(\text{tmd})$ in CDCl_3 .

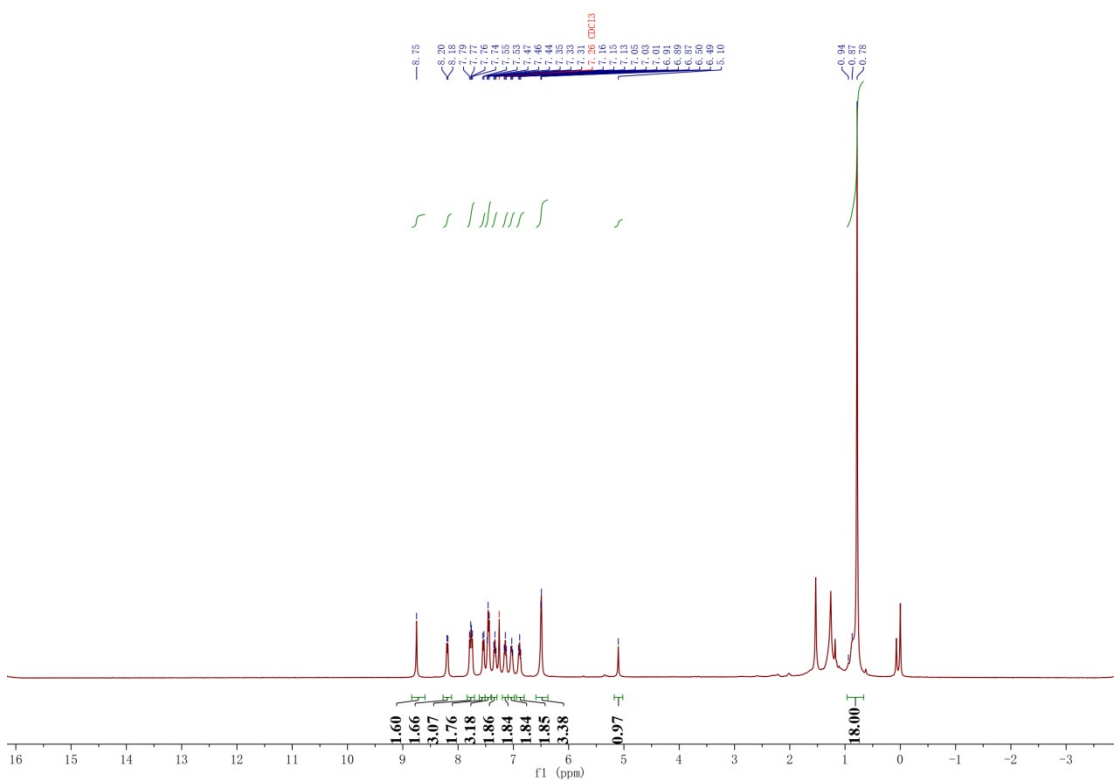


Fig. S7 ^1H NMR spectrum of $(\text{thzICz})_2\text{Ir}(\text{tmd})$ in CDCl_3 .

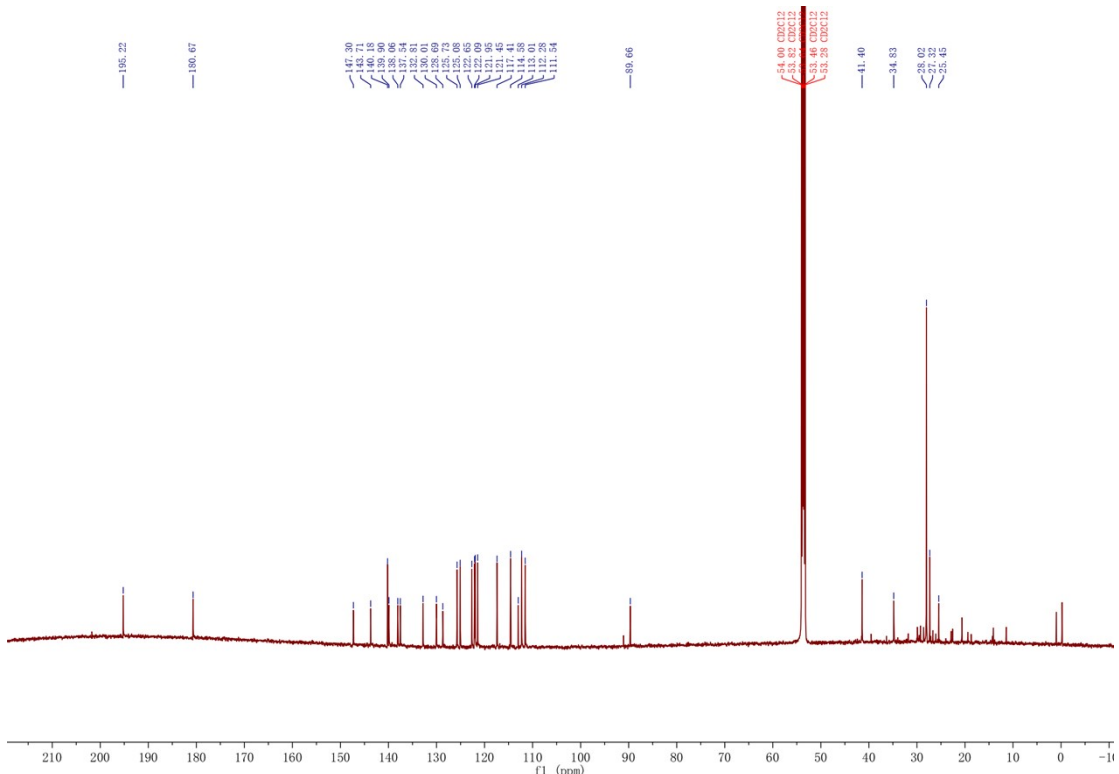


Fig. S8 ^{13}C NMR spectrum of $(\text{thzICz})_2\text{Ir}(\text{tmd})$ in CDCl_3 .

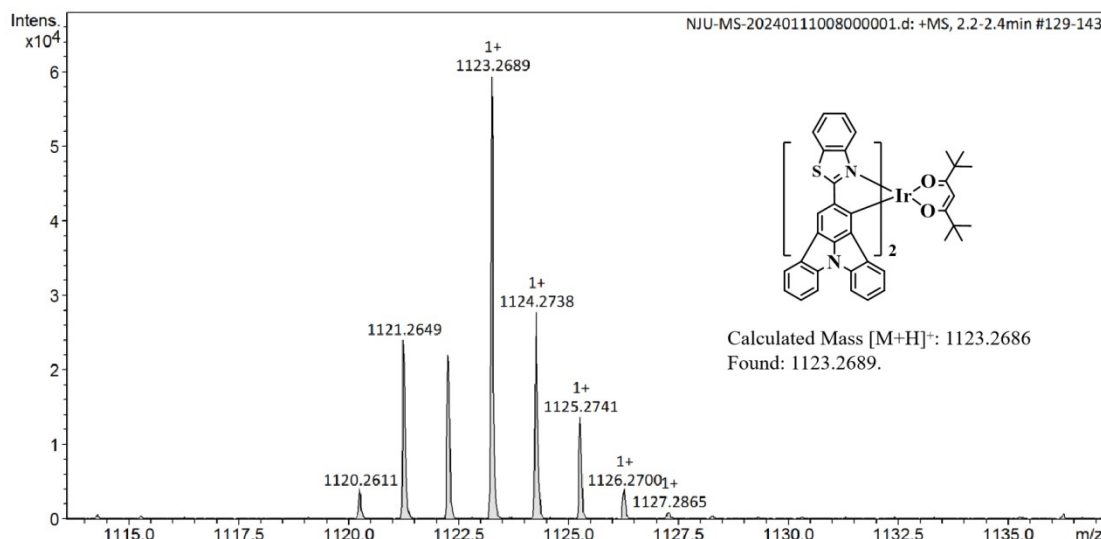


Fig. S9 HRMS spectrum of $(\text{PhthzICz})_2\text{Ir}(\text{tmd})$.

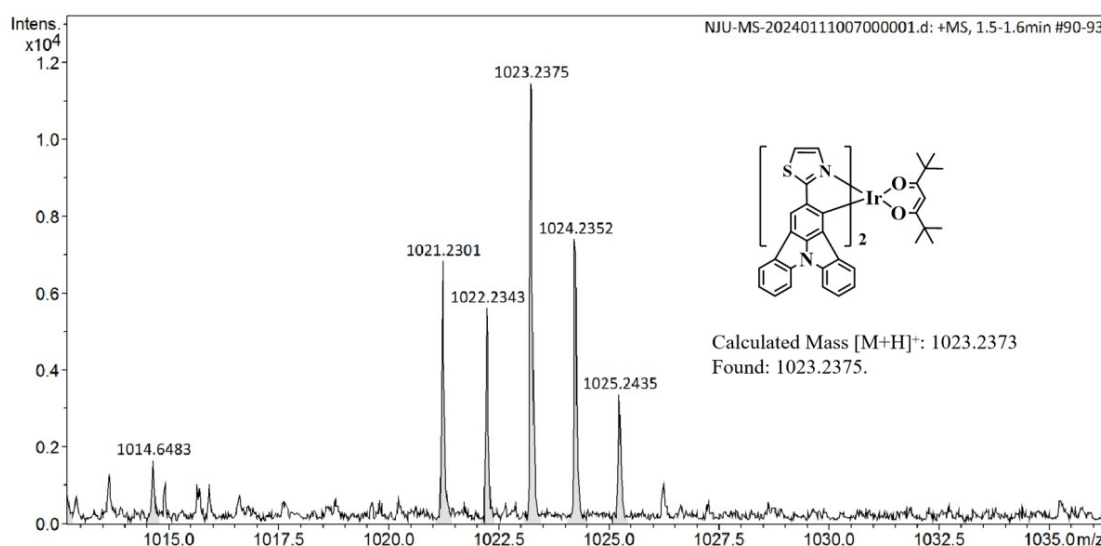


Fig. S10 HRMS spectrum of $(\text{thzICz})_2\text{Ir}(\text{tmd})$.

S4. X-ray crystallographic data

Table S1. The crystallographic data of $(\text{PhthzICz})_2\text{Ir}(\text{tmd})$ and $(\text{thzICz})_2\text{Ir}(\text{tmd})$.

Complex	$(\text{PhthzICz})_2\text{Ir}(\text{tmd})$	$(\text{thzICz})_2\text{Ir}(\text{tmd})$
Formula	$\text{C}_{61}\text{H}_{45}\text{IrN}_4\text{O}_2\text{S}_2$	$\text{C}_{53}\text{H}_{41}\text{IrN}_4\text{O}_2\text{S}_2$
Formula weight	1122.33	1022.22
T (K)	193.0	193.0
Wavelength (Å)	1.34139	1.34139
Crystal system	triclinic	monoclinic
Space group	P_{-1}	C_2/c
a (Å)	16.2630(8)	16.8239(11)
b (Å)	16.9870(9)	15.1822(10)

<i>c</i> (Å)	21.3893(11)	19.1241(12)
α (deg)	89.937(3)	90
β (deg)	85.461(3)	92.412(2)
γ (deg)	81.121(2)	90
<i>V</i> (Å ³)	5819.5(5)	4880.4(5)
<i>Z</i>	4	4
$\rho_{\text{calculated}}$ (g/cm ³)	1.281	1.391
μ (Mo K α) (mm ⁻¹)	3.600	4.256
<i>F</i> (000)	2256.0	2048.0
Range of transm factors (deg)	3.606 to 107.96	6.826 to 107.974
Reflns collected	85178	25937
Unique(R _{int})	21110(0.0519)	4435(0.0496)
R_I^a , wR_2^b [$I > 2s(I)$]	0.0359, 0.0886	0.0240, 0.0649
R_I^a , wR_2^b (all data)	0.0521, 0.0957	0.0259, 0.0669
GOF on F^2	1.078	1.071
CCDC NO	2344113	2344117

$$R_I^a = \Sigma ||F_o| - |F_c|| / \Sigma F_o. \quad wR_2^b = [\Sigma w(F_o^2 - F_c^2)^2 / \Sigma w(F_o^2)]^{1/2}$$

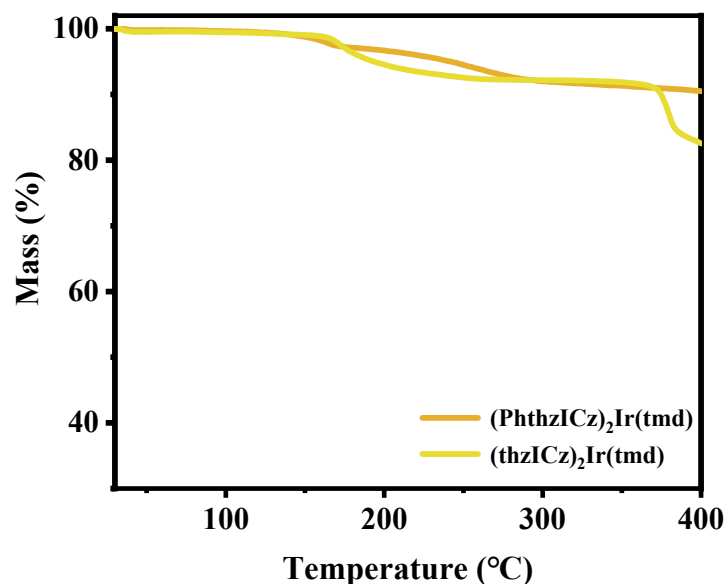
Table S2. Selected bond lengths and angles of (PhthzICz)₂Ir(tmd).

Selected Bonds	Bond length (Å)
Ir1-O1	2.132(3)
Ir1-O2	2.125(3)
Ir1-N2	2.024(3)
Ir1-N4	2.052(3)
Ir1-C18	2.004(4)
Ir1-C35	1.990(4)
Selected angles	(°)
O2-Ir1-O1	87.09(10)
N2-Ir1-O1	82.35(11)
N2-Ir1-O2	96.23(11)
N2-Ir1-N4	173.97(12)
N4-Ir1-O1	98.15(11)
N4-Ir1-O2	77.81(11)
C18-Ir1-O1	85.22(13)
C18-Ir1-O2	171.84(13)
C18-Ir1-N2	80.05(14)
C18-Ir1-N4	105.97(14)
C35-Ir1-O1	174.91(13)
C35-Ir1-O2	87.84(13)
C35-Ir1-N2	98.56(14)
C35-Ir1-N4	80.41(14)
C35-Ir1-C18	99.87(15)

Table S3. Selected bond lengths and angles of $(\text{thzICz})_2\text{Ir}(\text{tmd})$.

Selected Bonds	Bond length (Å)
Ir1-O1 ¹	2.121(19)
Ir1-O1	2.121(19)
Ir1-N2 ¹	2.017(2)
Ir1-N2	2.017(2)
Ir1-C16 ¹	2.004(3)
Ir1-C16	2.004(3)
Selected angles	(°)
O1-Ir1-O1 ¹	88.83(10)
N2-Ir1-O1 ¹	91.34(9)
N2 ¹ -Ir1-O1	91.35(9)
N2-Ir1-O1	84.59(9)
N2 ¹ -Ir1-O1 ¹	84.59(9)
N2 ¹ -Ir1-N2	174.32(12)
C16 ¹ -Ir1-O1 ¹	86.64(9)
C16 ¹ -Ir1-O1	171.71(9)
C16-Ir1-O1	86.64(9)
C16-Ir1-O1 ¹	171.71(9)
C16 ¹ -Ir1-N2	102.44(10)
C16-Ir1-N2	81.33(10)
C16-Ir1-N2 ¹	102.44(10)
C16 ¹ -Ir1-N2 ¹	81.33(10)
C16 ¹ -Ir1-C16	98.67(15)

S5. Thermal stability

**Fig. S11** TGA curves of Ir(III) complexes.

S6. Photophysical measurement

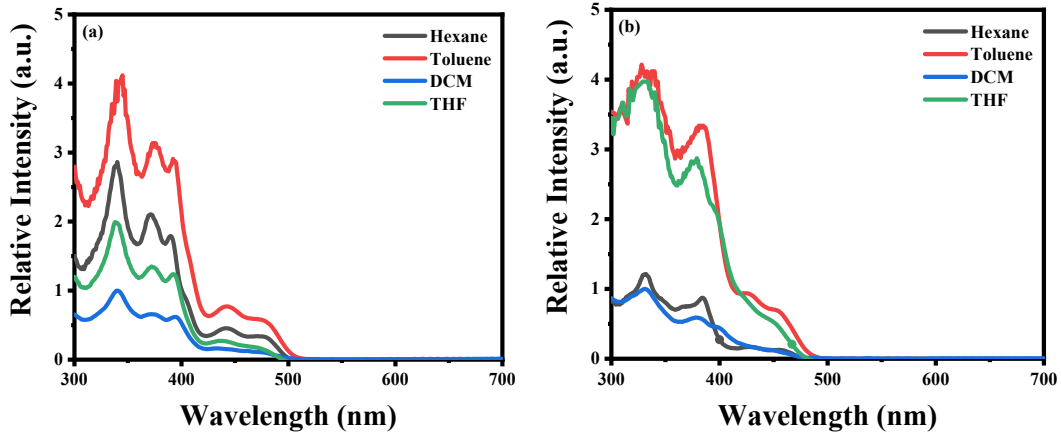


Figure. S12 Absorption spectra of (a) $(\text{PhthzICz})_2\text{Ir}(\text{tmd})$ and (b) $(\text{thzICz})_2\text{Ir}(\text{tmd})$ solvents with different polarities.

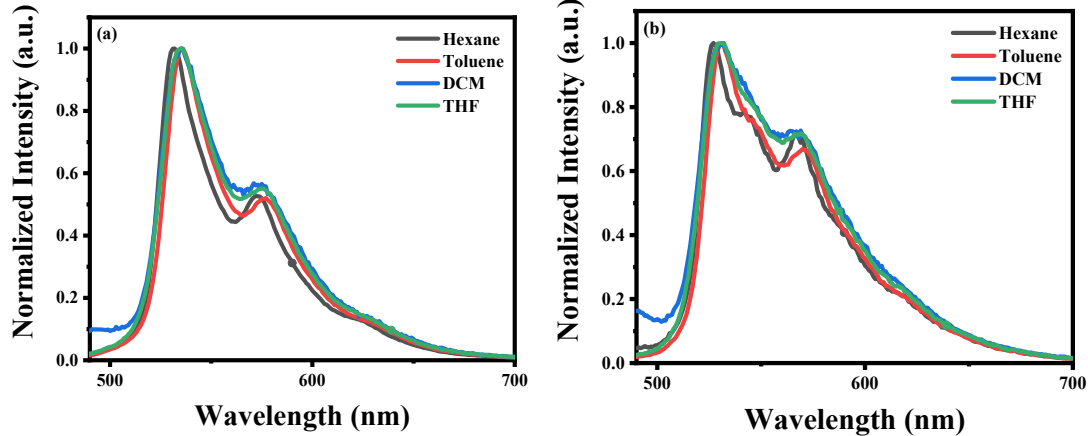
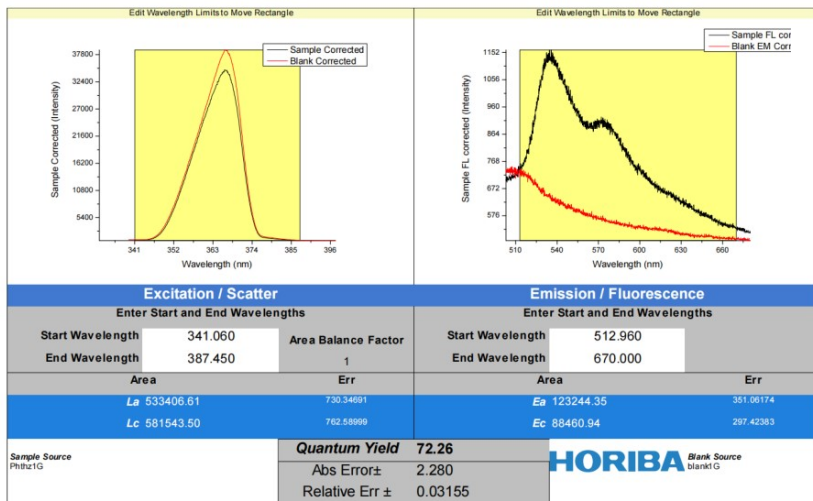


Figure. S13 Normalized PL spectra of (a) $(\text{PhthzICz})_2\text{Ir}(\text{tmd})$ and (b) $(\text{thzICz})_2\text{Ir}(\text{tmd})$ in solvents with different polarities at 298 K.



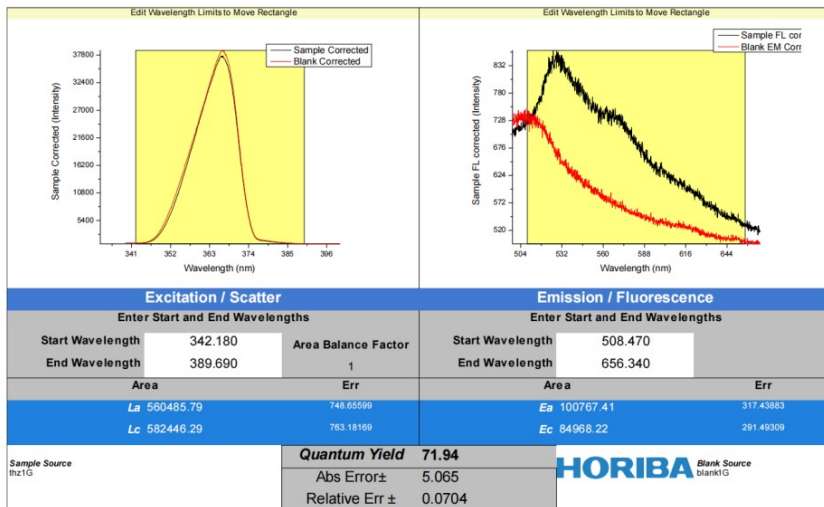


Fig. S14 PLQYs of Ir(III) complexes in deoxygenated DCM solutions (10^{-5} M).

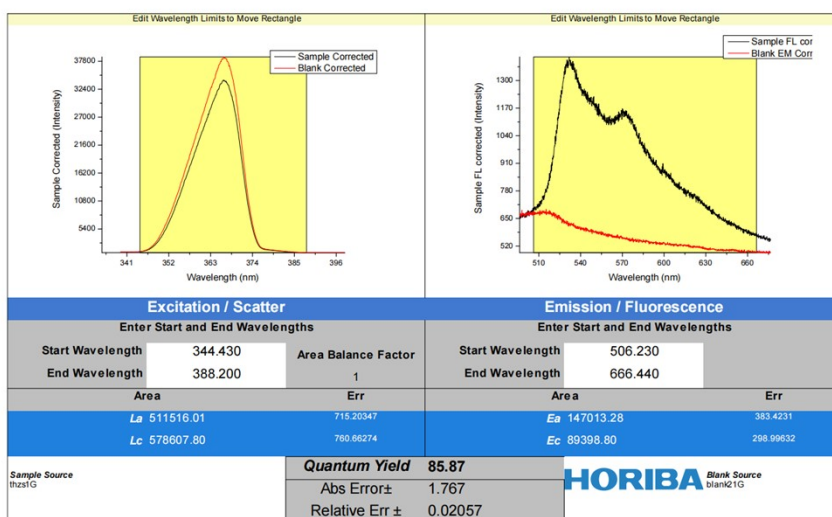
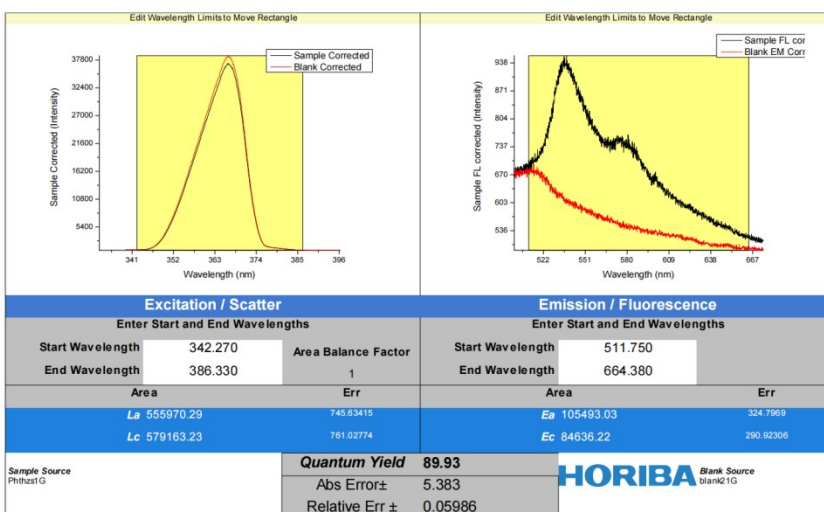


Fig. S15 PLQYs of Ir(III) complexes in doped films (5 wt% in mCBP).

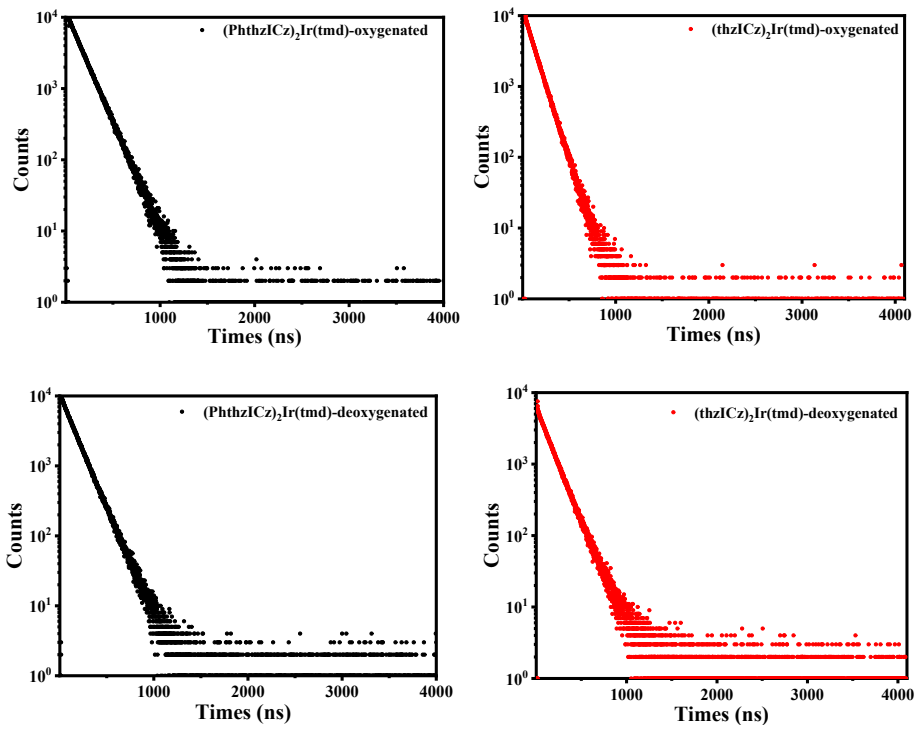


Fig. S16 Phosphorescence lifetime curves of Ir(III) complexes in oxygenated and deoxygenated DCM solutions (10^{-5} M).

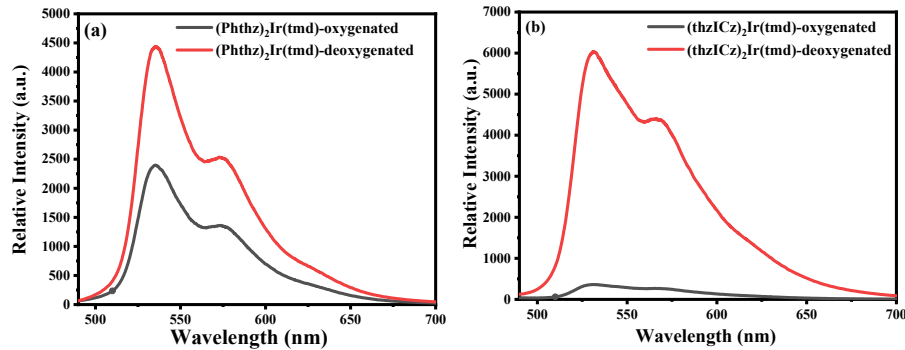


Fig. S17 Relative PL intensities of Ir(III) complexes in oxygenated and deoxygenated DCM solutions (10^{-5} M).

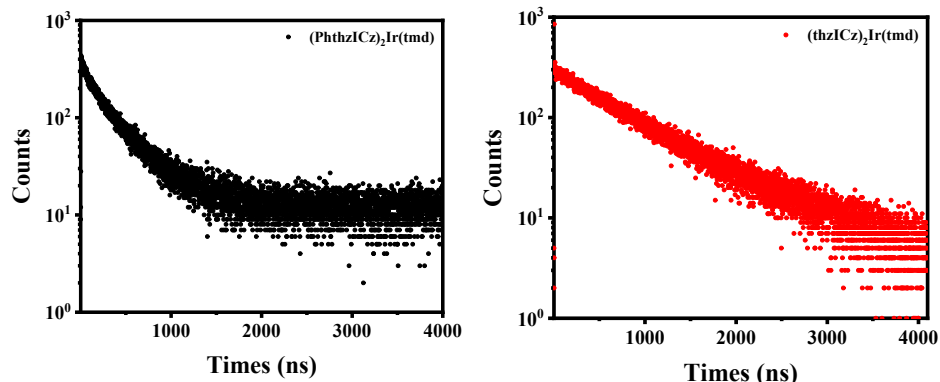


Fig. S18 Phosphorescence lifetime curves of Ir(III) complexes in doped films (5 wt% in mCBP).

S7. Electrochemical measurement

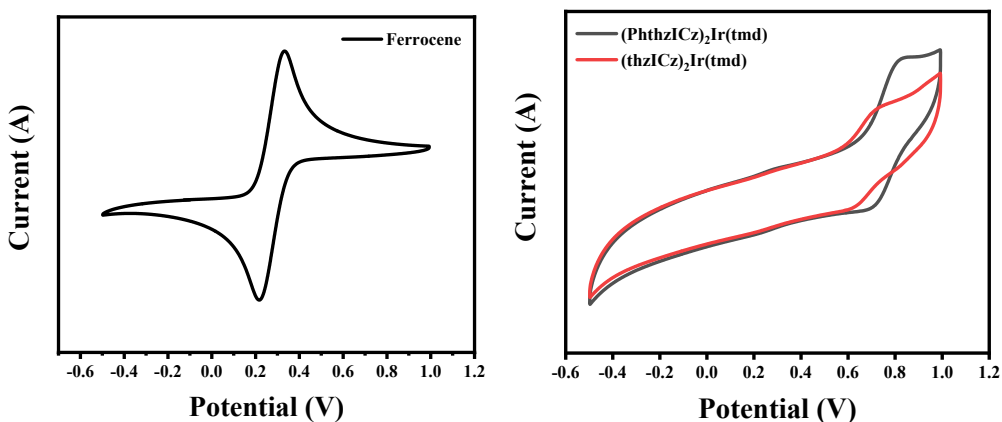


Fig. S19 CV curves of Fc and two Ir(III) complexes in deoxygenated CH_3CN solutions (10^{-5} M).

S8. Theoretical calculations

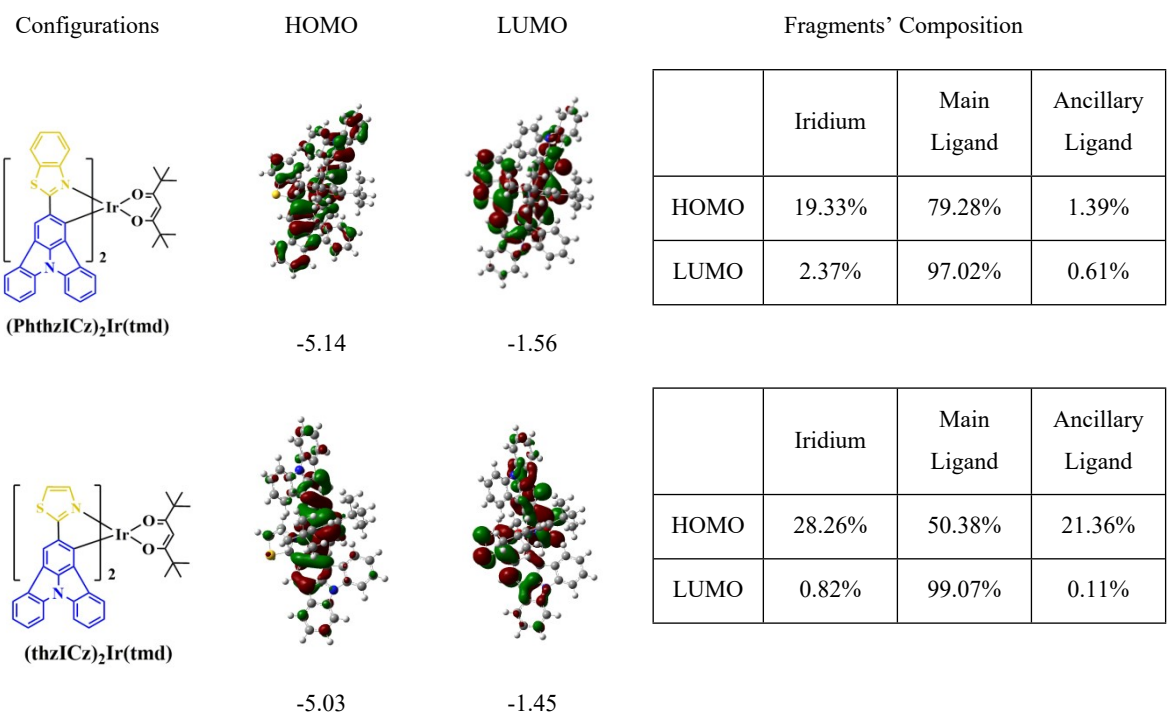


Fig. S20 Electron cloud distributions, HOMO/LUMO diagrams, and composition of each fragment of Ir(III) complexes obtained from theoretical calculations.

Table S4. TD-DFT calculations with IFCT method of $(\text{PhthzICz})_2\text{Ir(tmd)}$.

Donor	Acceptor		
	Iridium	Ancillary ligand	Main ligand
Iridium	0.004	0.001	0.179
Ancillary ligand	0.000	0.000	0.021
Main ligand	0.017	0.004	0.774

Table S5. TD-DFT calculations with IFCT method of $(\text{thzICz})_2\text{Ir}(\text{tmd})$.

Donor	Acceptor		
	Iridium	Ancillary ligand	Main ligand
Iridium	0.003	0.000	0.144
Ancillary ligand	0.000	0.000	0.018
Main ligand	0.017	0.003	0.813

S9. Electroluminescence measurement

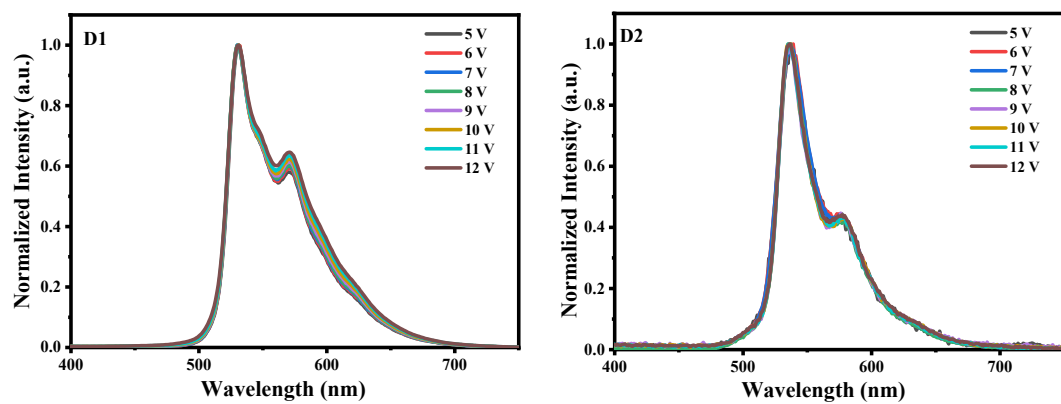


Fig. S21 EL spectra of D1 and D2 taken at different voltages from 5 to 12 V.